The Astrophysical Journal, 591:1203–1209, 2003 July 10
© 2003. The American Astronomical Society. All rights reserved. Printed in U.S.A.

ONSET OF MASS LOSS IN RED GIANTS: ASSOCIATION WITH AN EVOLUTIONARY EVENT

D. J. Mullan
Bartol Research Institute, University of Delaware, Newark, DE 19716; mullan@bartol.udel.edu

and

J. MacDonald
Department of Physics and Astronomy, University of Delaware, Newark, DE 19716; jimmacd@udel.edu
Received 2002 October 18; accepted 2003 March 19

ABSTRACT

Stencel & Mullan used asymmetries in the Mg II *k* emission line profile to determine the location of a "velocity dividing line" (VDL) in the H-R diagram. Stars to the right of (and above) the VDL were observed to have asymmetries that are consistent with the presence of cool massive winds. Stars to the left of (and below) the VDL showed no evidence for winds. We show that the VDL lies close to a certain event of stellar evolution on the red giant branch (RGB). The event occurs when the hydrogen-burning shell evolves outward through a discontinuity in molecular weight. In some low-mass stars, this event causes a kink in the evolutionary track of an individual low-mass star. In a cluster, the combined effects of such kinks create a "bump" in the luminosity function. Our result suggests that evolution through the kink (or bump) on the RGB is associated with the onset of a cool massive wind. Theoretical possibilities to explain this association will be explored in a subsequent paper.

Subject headings: stars: evolution — stars: magnetic fields — stars: mass loss

1. INTRODUCTION

The presence of "dividing lines" in the H-R diagram, separating regions where stars have distinct atmospheric properties, started when *IUE* was able to observe transition region (TR) lines in various stars (Linsky & Haisch 1979). The possibility that dividing lines might exist not only in TR lines, but also in velocity and in X-rays was explored by many authors in the 1980s and early 1990s.

A "velocity dividing line" (VDL) was discovered by Stencel & Mullan (1980a, 1980b) on the basis of *IUE* data. The key observational signature that is used in defining the VDL is an asymmetry in the double-peaked profile of the *h* and *k* emission cores of Mg II. Quantitatively, the asymmetry is defined in terms of the ratio of the intensity of the short-wavelength peak (S) to the intensity of the long-wavelength peak (L). In the Sun (observed as a star), the ratio of S/L is larger than unity, but in many cool giants and supergiants, S/L has a value that is less than 1, sometimes considerably less. Stencel & Mullan suggested that a low S/L value indicates the presence of a cool massive wind.

Stencel & Mullan (1980a) reported on measurements of the S/L ratio in a sample of several dozen field stars. Because interstellar absorption may corrupt the S/L ratio, Stencel & Mullan (1980b, hereafter SM80) considered a restricted sample of 19 stars in which the interstellar effects are not expected to affect the measured S/L ratio. They found that when these stars were plotted in an H-R diagram, a clear line of demarcation could be drawn between stars with $S/L < 1$ (in the upper right) and stars with $S/L > 1$ (in the lower left). SM80 interpreted the line of demarcation (which lies in the red giant region) as a "velocity dividing line" (VDL).

If a change in the sense of the asymmetry of the *h* and *k* emission cores was all that happened in crossing the VDL, one might perhaps regard the SM80 result as merely a quirk of the Mg II lines (due, e.g., to radiation transfer effects in the increasingly spherical geometry as a star ascends the red giant branch [RGB]). However, it is essential to note that other well-defined changes *are* in fact also observed in the outer atmospheres of cool giants near the VDL. Specifically, SM80 pointed out that the VDL lies close to the "temperature dividing line" discovered by Linsky & Haisch (1979) in TR lines. Subsequently, X-ray data also suggested that coronal emission essentially disappears in the H-R diagram when stars crosses a "coronal dividing line" (Ayres et al. 1981; Haisch, Schmitt, & Fabian 1992), which lies close to the VDL of SM80.

These results indicate that when a red giant evolves across the VDL, there is a clear tendency for the hot corona to disappear and for a cool massive wind to set in. It appears unlikely, therefore, that the VDL can be dismissed simply as a quirk of radiative transfer in Mg II. On the contrary, in the vicinity of the VDL, a process apparently occurs that alters in a significant manner the physical properties of the outer atmosphere of a red giant star.

Although various theoretical ideas have been proposed for such a process (typically involving magnetic restructuring; e.g., Mullan 1983; Rosner et al. 1995), we will postpone a discussion of magnetic effects to a later paper. Here, we focus on a simpler aspect of the problem, namely, a possible interpretation of the location of the VDL in light of stellar evolution theory.

2. UPDATE ON THE LOCATION OF THE VDL IN THE H-R DIAGRAM

On a historical note, we should point out that SM80 used the width of the Mg II *k* line as a measure of absolute magnitude, $M_V(k)$. At that time, this process (an analog of the Wilson-Bappu effect in the Ca II H and K lines) was believed to be a reliable method of determining stellar distances.

However, in the intervening years, *Hipparcos* distances have become available for all of the stars in the SM80 sample. The *Hipparcos* data indicate that although in most cases

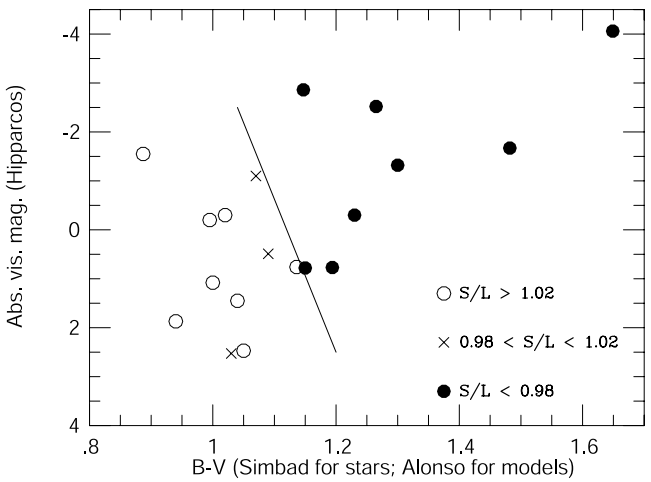


FIG. 1.—Asymmetry in the emission peaks of the Mg II *h* and *k* lines as a function of position in the H-R diagram. (This figure is an update of Fig. 1 in SM80.) *Filled circles*: Stars with S/L < 1 and negative radial velocity; these stars are considered to have cool massive winds. *Open circles*: Stars with S/L > 1 and positive radial velocity; these stars have solar-like coronae and undetectable winds. *Crosses*: Stars with S/L close to unity.

the "Wilson-Bappu" magnitudes used by SM80 were fairly good, there were some exceptions. The most notable exceptions are 56 Peg, with an error of −4 mag [$M_V(k) = -5.3$; $M_V(Hipp) = -1.32$], and α UMa, with an error of +2.5 mag [$M_V(k) = +1.4$; $M_V(Hipp) = -1.10$].

A revised version of the figure in SM80 (now using only *Hipparcos* distances) is shown in Figure 1. As part of the revision, and for convenience in comparing with evolutionary tracks later, we use $B-V$ for the abscissa, rather than $V-R$ as used by SM80. (No essential differences would appear in the figure if we were to use $V-R$ as abscissa.) We see that the data can be divided plausibly into three groups. Group I (*filled circles*) consists of eight stars in which S/L is clearly less than 1: stars in this group tend to lie toward the upper right. Group II (*open circles*) consists of eight stars in which S/L is clearly in excess of 1: stars in this group tend to lie toward the lower left. Group III (*crosses*) consists of three stars in which S/L is close to unity: two of these stars lie in an intermediate position between groups I and II.

Although some of the individual points plotted in Figure 1 have moved compared to their plotted positions in SM80, we see that there is a still a rather clean separation between the two groups of stars. Thus, the SM80 suggestion concerning the existence of a VDL persists in the revised data.

We have plotted in Figure 1 one possible estimate of where a revised VDL might be drawn. Quantitatively, our choice of revised VDL starts at around $M_V = +2$ (with $B - V \approx 1.15$) and goes up through $M_V = 0$ (with $B - V \approx 1.1$) toward $M_V = -2$ (with $B - V \approx 1.05$). The range of absolute magnitudes estimated here, roughly +2 to −2, will be important in what follows.

3. QUANTITATIVE INTERPRETATION OF S/L

SM80 ascribed low values of S/L to the outflow of a massive cool wind. If such a wind exists, it will preferentially scatter blue photons, thereby reducing S/L to values below unity. For a strong line such as the Mg II *k* line, it might be expected that even a weak wind (with relatively low mass-loss rate) might give rise to significant absorption of the S peak. At the time of the Stencel-Mullan work, there was no quantitative analysis available that would allow one to go beyond this qualitative discussion. As a result, SM80 did not use their data to evaluate the mass-loss rates. To the extent that the VDL in Figure 1 is in fact a sharp boundary, the conclusion of SM80 remained essentially qualitative: the onset of the cool massive winds occurs quite abruptly in the H-R diagram.

However, in the years that have elapsed since the work of SM80, a tool for quantitative analysis of mass-loss rates based on Mg II *k* line profiles has become available (Robinson, Carpenter, & Brown 1998). Using a method known as SEI (Sobolev with exact integration), Robinson et al. have been able to reproduce successfully the profiles of several lines (due to magnesium, oxygen, and iron) that are scattered by the wind. In the K5 III stars α Tau and γ Dra, where S/L ≈ 0.5 and 0.4, respectively, Robinson et al. have determined that the mass-loss rates are of order $10^{-11}\ M_\odot\ \mathrm{yr}^{-1}$. These mass-loss rates are at least 100 times larger than the solar mass-loss rate. Moreover, the fact that the wind can scatter Mg II photons strongly indicates that the winds are much cooler than the solar wind. Thus, an up-to-date interpretation of the VDL in Figure 1 points to the onset of cool winds with mass-loss rates of order $10^{-11}\ M_\odot\ \mathrm{yr}^{-1}$ among cool giant stars with $M_V \approx -2$ to +2, and with $B - V \approx 1.05$–1.15.

To be sure, the mass-loss rates reported by Robinson et al. 1998 for the two K5 giants are relatively small compared to those from (say) OB stars, or from the coolest red supergiants, but it is an indication of the great sensitivity of the S/L ratio that even winds as weak as $10^{-11}\ M_\odot\ \mathrm{yr}^{-1}$ can be detected by observing the Mg II *h* and *k* lines. Note that the Ca II H and K lines are not as well suited to this problem: their line widths are too narrow to be useful for detecting the cool wind that sets in at the VDL (Mullan 1984).

4. THE "BUMP" ON THE RGB: EMPIRICAL

When empirical luminosity functions are constructed for stars on the RGB in a cluster, a local maximum in the (differential) distribution occurs at a certain absolute magnitude. This local maximum is referred to as the "bump."

According to evolutionary models, the bump occurs at a well defined absolute magnitude that depends on age and metallicity. For example, at an age of 15 Gyr, Cassisi & Salaris (1997) obtained isochrones that yield

$$M_V^{\mathrm{bump}} = 2.212 + 1.768[\mathrm{M/H}] + 0.294[\mathrm{M/H}]^2 ,$$

while Ferraro et al. (1999) propose the following age-dependent expression for a cluster of age t_9 Gyr:

$$M_V^{\mathrm{bump}} = 0.7502 + 0.9896 \log t_9 + 1.5797[\mathrm{M/H}] + 0.2574[\mathrm{M/H}]^2 .$$

In both of these expressions, the metal abundance term [M/H] includes information about not only [Fe/H] but also an enhancement in α-elements.

When we turn to the field stars in the solar neighborhood, we are no longer dealing with a coeval population. Therefore, we do not expect that estimates of M_V^{bump} derived from isochrones will be precisely applicable. However, the second expression above might provide some guidance to the

expected bump brightness in the solar neighborhood. Setting [M/H] to zero (appropriate to Population I stars), and considering ages within a factor of (say) 2 of the Sun (i.e., with $\log t_9 \approx 0.4$–0.9), we see that the bump might lie in the range $M_V^{\rm bump} = +(1.1$–$1.6)$. In fact, for a sample of field stars, Charbonnel & Do Nascimento (1998) suggest that the bump region lies in the range $0 \leq M_V \leq 2$.

We note that this range overlaps with the location of our estimated "dividing line" in Figure 1. This overlap suggests that we explore the following hypothesis: the onset of massive cool winds may be connected with the evolution of a star through the bump. In order to determine whether or not there is a physical underpinning for such a connection, we need to consider in some detail what happens to a star at the bump.

5. THE BUMP ON THE RED GIANT BRANCH: THEORETICAL

The physical origin of the bump is well understood: in fact, its existence was a "genuine prediction of theory" (Salaris, Cassisi, & Weiss 2002), originating in papers by Thomas (1967) and Iben (1968). In order to set the stage for a (future) theoretical understanding of why the bump might be related to mass loss, it is important that we describe in some detail what happens to the internal structure of a star at the bump.

When a star with relatively low mass (less than a few solar masses) evolves off the main sequence, the convective envelope grows in depth, penetrating more and more deeply below the surface of the star. However, at a certain point in evolution, the depth of the convective envelope reaches a maximum value. As Salaris et al. (2002) write, "convection reaches its maximum extension (in mass) near the base of the RGB, and from this moment on, the lower convective boundary slowly recedes toward the surface." In an unprocessed convective envelope, hydrogen abundances remain at their initial value. Therefore, there is a sharp discontinuity in the H profile that remains behind at radial distance R_d (or at mass coordinate M_d): this discontinuity indicates the level of maximum penetration of the envelope.

The sense of the discontinuity is as follows: on the side closer to the surface, $X_{\rm H}$ (the hydrogen abundance by mass) is large and its radial profile is flat, while on the side closer to the center of the star, $X_{\rm H}$ is distinctly smaller and falls off in value toward the center of the star. For example, Cassisi, Salaris, & Bono (2002) illustrate an example in which $X_{\rm H} = 0.74$ throughout the envelope (where $M/M_{\rm tot} > 0.265$), while just inside $M/M_{\rm tot} = 0.265$, $X_{\rm H}$ falls discontinuously to 0.60. Between $M/M_{\rm tot} = 0.265$ and 0.23, $X_{\rm H}$ decreases from 0.60 to 0.56. Inside the helium core ($M/M_{\rm tot} \leq 0.23$), $X_{\rm H}$ falls precipitously to zero.

Two alterations are noteworthy at M_d. First, the magnitude of the mean molecular weight μ is smaller above M_d than below. Second, the radial gradient of μ has a nonzero value below M_d, but above M_d, the radial gradient of μ is zero. The second of these is an important feature to which we will return.

The evolutionary consequences of the discontinuity at R_d are clear. As a star evolves up the RGB, the growing He core pushes the H-burning shell farther out, and at some point in evolution, the H shell encounters the discontinuity at M_d. Suddenly, the H shell finds itself with access to an enhanced supply of fuel. According to Salaris et al. (2002), "The star reacts to the sudden increase in available fuel by lowering its surface luminosity and slowing down the evolutionary timescale, before starting again to increase its luminosity after the shell has moved past the discontinuity."

The temporary decrease in luminosity appears as a zigzag or "kink" on the evolutionary track of a low-mass giant: instead of continuing to progress up along the RGB toward higher luminosities, the low-mass star temporarily regresses to a lower luminosity, with a slightly bluer color. Because of the reduced luminosity, the rate of evolution of the star slows down. After a short time interval, the star then resumes its progress up along the RGB toward higher luminosity.

The magnitude of the kink is greatest in stars of the lowest mass. However, even in the case of a 1 $M_\odot$ star, the kink is small enough that it is easily missed in a casual inspection of an evolutionary track. In Figure 2 we show an expanded version of the evolutionary track of a 1 $M_\odot$ star with $Z = 0.02$. The temporary decrease in luminosity at the kink amounts to about 0.05 mag in M_v, and the displacement in color between the RGB track before and after the kink is about 0.005 mag in $B-V$. An expanded view of a kink can also be found in Cassisi et al. (2002; their Fig. 4).

The slowing down in evolution results in a local maximum in the differential luminosity function: this gives rise to the bump. Thus, the kink on the track of an individual star creates a bump when we examine a cluster of coeval stars. As a result, we use the terms "kink" and "bump" interchangeably. Because the evolutionary effects are relatively slight, a cluster must contain many stars if the bump is to be identified with good statistical significance. According to Ferraro et al. (2000), there must be at least 2000 RGB stars within 3 mag of the RGB tip. Despite this requirement that a cluster must be relatively rich in stars, a localized bump has in fact been clearly identified in several dozen globular clusters using either ground-based or space-based data (Ferraro et al. 1999; Zoccali et al. 1999). The clusters in the sample have metal abundances that vary over a range of

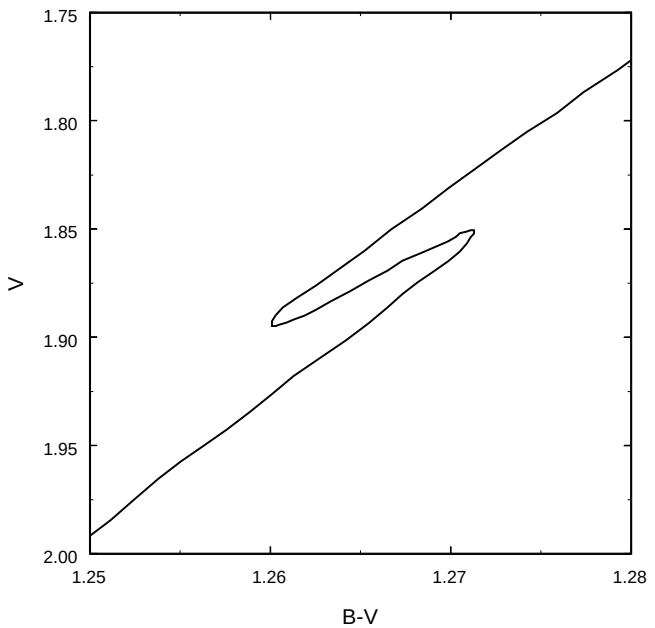


FIG. 2.—Expanded view of the kink in the evolutionary track of a 1 $M_\odot$ star with $Z = 0.02$.

almost 2 orders of magnitude. Theoretical predictions of bump luminosity fit the data well.

For our purposes, we note that the bump marks a point in a star's evolution where the H shell passes from a region where $d\mu/dr$ is nonzero to a region where $d\mu/dr$ is zero. A clear bump appears only on the evolutionary tracks of stars with masses up to a certain limit: this limit depends on Z. For solar abundances, the kink remains identifiable as a distinct entity up to masses of about 2.25 $M_\odot$. In stars more massive than about 2.5 $M_\odot$, He core burning begins *before* the H-burning shell reaches the μ discontinuity. Because He burning is already contributing a dominant portion to the luminosity at this point, the localized change in H-shell burning is swamped, and is almost undetectable as far as the luminosity of the star is concerned. This results in no apparent bump on the track.

Nevertheless, we stress that the physical process that we remarked on in the lower mass stars *still takes place*: namely, the H shell still (at some point during evolution) does undergo a transition from a region where $d\mu/dr$ is nonzero to a region where $d\mu/dr$ is zero. We speculate that this transition in $d\mu/dr$ may play a key role in the physics of the dynamo: this could be important for understanding why coronal structure changes abruptly at the bump. (We postpone a discussion of this speculation to a future paper.)

It just so happens that in low-mass stars, the luminosity of the star provides us with an externally visible marker that such a transition is occurring deep inside the star. In more massive stars, the physical transition across the μ discontinuity still occurs at a certain point, even though we no longer have the luxury of a marker in luminosity to highlight the event. If the physical process that controls the rate of mass loss is connected in some way with the transition in $d\mu/dr$, then the physics will be similar whether or not the star has a detectable bump on its evolutionary track.

6. THE BUMP IN RELATION TO MASS LOSS ONSET: EVOLUTIONARY TRACKS

In order to determine more quantitatively whether the onset of mass loss in the SM80 sample is related to the bump, we have calculated evolutionary tracks for a range of stellar masses and for various metal abundances.

To compute models of stars that pass through the region of the H-R diagram discussed by SM80, we use MacDonald's stellar evolution code (JMSTAR). This code has been developed from an early version of a code of Peter Eggleton's, and it allows us to calculate the evolution of a star from an initial pre–main-sequence model up to and past the helium flash at the tip of the RGB. We summarize the code briefly here. (For more details, see Jimenez & MacDonald 1996 and Mullan & MacDonald 2001.) The code is based on a Henyey approach, where the entire star is divided into 400–800 concentric shells including boundaries at center and surface. During the various stages of evolution, the grid of shells is allowed to evolve using an adaptive mesh technique. This requires an extra pair of differential equations that describe how changes in the variables across a shell are to be controlled. The adaptive mesh technique is particularly essential in order to resolve the discontinuity in molecular weight, which is so essential to the physics of the bump that we consider in this paper.

The current version of the code uses OPAL opacities (Iglesias & Rogers 1996) for temperatures greater than 7000 K. At lower temperatures, we evaluate Rosseland mean opacities by interpolating with respect to $\log T$ and $\log R'$ (where $R' \equiv \rho/T^3$) in table of opacities kindly supplied upon request by David Alexander for a discrete set of metal abundances: $Z = 0.0002$, 0.0005, 0.001, 0.004 (all with $Y = 0.24$), and $Z = 0.01$, 0.02, 0.05, 0.10 (with $Y = 0.235 + 2Z$). Nuclear reaction rates are mostly taken from Angulo et al. (1999).

At each point of a track for a given Z, the luminosity and effective temperature are converted to M_V and $B - V$ using the metal-dependent expressions given by Alonso, Arribas, & Martinez-Roger (1999).

As described above, we find that the tracks of low-mass stars, with masses up to 2.25 $M_\odot$ and with solar abundances, each exhibits a clearly defined kink on the RGB. Stars more massive than 2.5 $M_\odot$ do not exhibit a clear kink on their track when the H shell passes through the μ discontinuity.

Now we turn to comparing the evolutionary tracks with the particular stars in the SM80 sample. Since we have access to a set of only three Z values, we group the stars in the SM80 sample into three subsets, according to their empirical Z values. We take the latter from the list of [Fe/H] values given by Taylor (1999), converting them to Z values according to $\log Z = \log(0.018) + [\mathrm{Fe/H}]$. Of the 19 stars in the SM80 sample, 15 have [Fe/H] values listed by Taylor (1999). We now use these 15 stars to compare with evolutionary tracks with different metallicities.

6.1. *The $Z = 0.004$ Group*

Based on the Taylor (1999) data, we assign two stars to a group that is to be compared with the $Z = 0.004$ tracks. These are α Boo ($Z = 0.0051$) and ξ Cyg ($Z = 0.0067$). In Figure 3, we show absolute visual magnitude M_V versus $B - V$ color derived from the evolutionary tracks for stars with $Z = 0.004$, and with masses $M/M_\odot = 1$, 1.5, 2, 2.5, 3, 4, and 5. Crosses denote where the bumps occur on the three lower mass tracks. On the scale that we use to plot Figure 3,

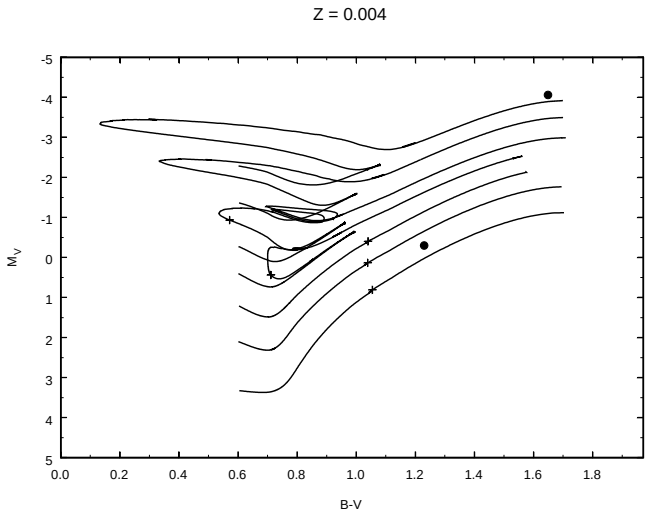


FIG. 3.—Evolutionary tracks for stars with $Z = 0.004$ and masses of 1, 1.5, 2, 2.5, 3, 4, and 5 $M_\odot$. On each track, a cross denotes the point at which the H-burning shell passes through the μ discontinuity. In stars with mass ≤ 2 $M_\odot$, a bump occurs at the location of the cross. Two stars in the SM80 sample with low metal abundance are plotted: both have S/L < 1 (indicating mass loss), and both lie above the bumps.

the bumps are so small that they are difficult to see: a detailed examination of the tracks is necessary (see Fig. 2 above for an example of a highly magnified bump.) On the higher mass tracks, a cross indicates where the H shell passes through the μ discontinuity, even if there is no longer a clear signature *in the luminosity* that this passage has occurred. Thus, all of the crosses in Figure 3 (as well as in subsequent figures) denote the transition of the H shell through the μ discontinuity, whether or not there is a kink in luminosity.

The filled circles in Figure 3 represent the two relevant stars in the SM80 sample, both of which have $S/L < 1$; i.e., both have detectable mass loss. For brevity we refer to stars with $S/L < 1$ as "mass losers," and we refer to stars with $S/L > 1$ as "non–mass losers." α Boo, at the lower luminosity ($M_v = -0.3$), lies between the tracks for 1 and 1.5 $M_\odot$. This is consistent with the published mass of α Boo: $1.1^{+1.7}_{-0.7}$ $M_\odot$ (Ayres & Johnson 1977). The crosses (i.e., bumps) on the 1 and 1.5 $M_\odot$ tracks can be seen to lie below and to the left of α Boo: therefore, α Boo has certainly evolved through the bump. The second star in Figure 3 (ξ Cyg: $M_v = -4.06$) is too luminous for it to be on a track with a visible bump, but it is so luminous that it has certainly evolved beyond the point where the H shell has passed through the μ discontinuity. Note that this star is also a mass loser.

6.2. *The $Z = 0.01$ Group*

Tracks for stars with $Z = 0.01$ are shown in Figure 4. For comparison with this group of tracks, we consider seven stars in the SM80 sample with Z ranging from 0.009 to 0.015. These are (in order to decreasing brightness) α Hya ($M_v = -1.67$; *filled circle*), ϵ Leo ($M_v = -1.55$; *open circle*), α UMa ($M_v = -1.10$; *filled circle*), ζ Hya ($M_v = -0.20$; *open circle*), ϵ Sco ($M_v = +0.78$; *filled circle*), 46 LMi ($M_v = +1.45$; *open circle*), and η Ser ($M_v = +1.87$; *open circle*). These seven stars are plotted in Figure 4, encoded (as before) in terms of their S/L value.

Only three of the seven stars in Figure 4 have small enough masses to lie on tracks with clearly defined bumps. Of these three stars, the two faintest (η Ser and 46 LMi) are plotted with open circles, indicating $S/L > 1$, i.e., no detectable mass loss. These stars lie close to the 1.5 $M_\odot$ track, and we note that both stars lie well *below* the bump on that track.

The next brightest star is ϵ Sco. It is plotted in Figure 4 with a filled circle, indicating $S/L < 1$; i.e., the star has detectable mass loss. We see that ϵ Sco lies almost exactly at the bump on the 1.5 $M_\odot$ track. Note that ϵ Sco is a suspected variable (NSV 7983), with V magnitude variable between 2.24 and 2.35. Therefore, depending on the phase of variability of the star when the S/L data were obtained, a more accurate plotting of ϵ Sco might shift the plotted symbol slightly above or slightly below the bump.

In the upper right corner of Figure 4, the star α Hya (also a mass loser; *filled circle*) lies between the tracks for masses of 2.5 and 3 $M_\odot$. For stars of either of these masses, the point where the H shell passes through the μ discontinuity (marked by crosses) lies far below the location of α Hya. Thus, α Hya has certainly evolved beyond the crosses.

Three other stars are also plotted in Figure 4: in order of decreasing brightness, they are ϵ Leo (no mass loss), α UMa (S/L close to unity, and variable), and ζ Hya (no mass loss). All three lie in the evolutionary region where blue loops are prominent. Here, it is difficult to identify with confidence the correct stellar mass on the basis of the evolutionary tracks. As a result, it is difficult to say definitively whether or not the H shell in the star has passed through the μ discontinuity (marked with a cross on each track).

6.3. *The $Z = 0.02$ Group*

Results are shown in Figure 5. Six stars from the SM80 sample are assigned to this group. Of these six, four are non–mass losers (*open circles*), and two are mass losers (*filled circles*). Two of the stars lie on tracks with bumps. The fainter of these (with $M_V = 2.5$) is ν_2 CMa. This star is a non–mass loser that lies on the 1.5 $M_\odot$ track, at a position well below the bump. The brighter of the two, β Oph (a mass loser), lies on the 2.0 $M_\odot$ track at a location somewhat below the bump. However, β Oph is a suspected variable

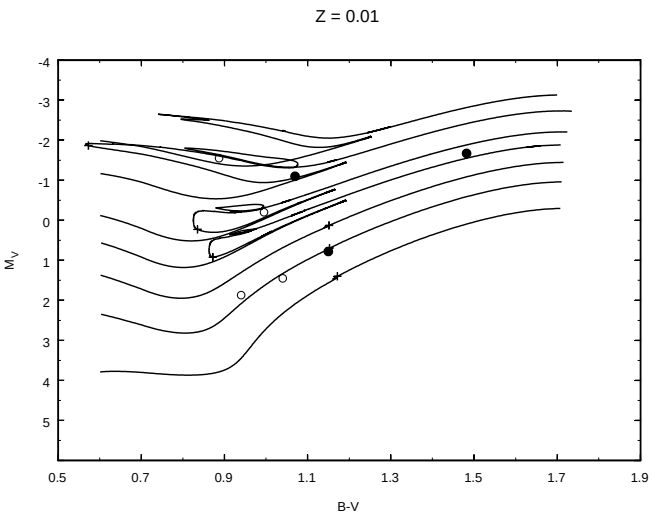


FIG. 4.—Evolutionary tracks for stars with $Z = 0.01$, plotted with the same notation as in Fig. 2. Stars in the SM80 sample with Z near 0.01 are plotted with filled circles (mass losers) and open circles (no detectable wind).

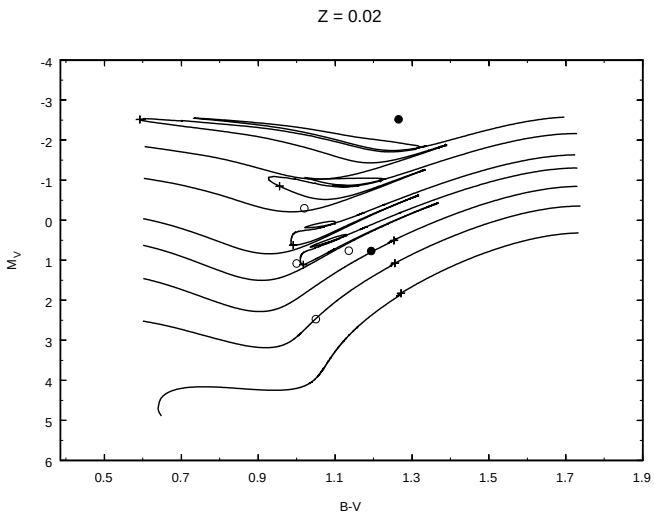


FIG. 5.—Evolutionary tracks for stars with $Z = 0.02$, plotted with the same notation as in Fig. 2. Stars in the SM80 sample with Z near 0.02 are plotted with filled circles (mass losers) and open circles (no detectable wind).

(NSV 23613), with V magnitude varying between 2.75 and 2.77. It is also a radial velocity variable, with multiple periods (0.237, 0.255, and 13 days; Henry et al. 2000). Depending on the phase of the variability cycle at which the S/L ratio was measured, β Oph might lie even closer to the bump. The other clear mass loser in Figure 5 (θ Lyr; *filled circle*) is so luminous that, even if we cannot pin down its mass well, the star certainly lies past the evolutionary stage where the H shell passes through the μ discontinuity.

There are three other non–mass losers (*open circles*) in Figure 5. Of these, the brightest, β Cet (with $M_v = -0.3$) lies close to the track for the 4 $M_\odot$ star. If this is indeed the correct mass of β Cet, then β Cet has not yet ascended the RGB, and has certainly not yet reached the cross on the 4 $M_\odot$ track. Similarly, for γ Com (at $M_v = +0.76$), it appears that the star lies closest to the 2.5 $M_\odot$ track: if its mass is indeed 2.5 $M_\odot$, then the star has not yet ascended the RGB, and has not yet evolved to the position of the cross on the track. The final star, β Gem (with $M_v = +1.08$) lies close to the cross on the 2.5 $M_\odot$ track: this star is a non–mass loser.

6.4. *Testing the "Bump Hypothesis"*

In this study, our aim has been to test the following hypothesis: a key role in mass loss is played by a certain event in evolution. This event occurs when the H shell evolves outward through the μ discontinuity. In low-mass stars this event causes a bump on the track. In more massive stars, there is no discernible bump. In all cases, we mark the event with a cross on the evolutionary track. For brevity, we refer to the event in both cases as the bump. With this notation, we restate the hypothesis that we wish to test: mass loss does *not* occur before the bump, but mass loss *does* occur at or above the bump. In what follows, we refer to this as the "bump hypothesis."

In the three groups that we have identified with different mean metal abundances (Figs. 3–5), we find six stars that lie on (or close to) tracks that contain identifiable bumps. Of these, we have identified three non–mass losers, all of which lie clearly *below* the bump, and two mass losers that lie *at or above* the bump. The sixth star (a mass loser), lies somewhat below the bump (although this might change if the known variability of the star can be accounted for). Thus, for the stars in this group, we find a success rate of at least 5 out of 6 for the bump hypothesis. As regards stars that are too massive to lie on tracks with bumps, we identify five such stars. For these five, we use the cross on the track as a proxy for the bump. We find that three of the five stars that have certainly evolved beyond the cross are mass losers. Our tracks suggest that the other two stars have not yet evolved to the cross: both these two are found to be non–mass losers. Therefore, testing the bump hypothesis among this group, we find a success rate of 5 out of 5. The remaining four stars lie on portions of evolutionary tracks where it is difficult to decide whether or not the star has passed the cross. It is therefore difficult to test the bump hypothesis for this group. In the worst case, the success rate could be as poor as 0 out of 4, whereas in the best case, it might be as good as 4 out of 4. Even with the worst case, the total success rate for the bump hypothesis is at least 10 out of 15. In the best case, it could be as high as (at least) 14 out of 15.

7. DISCUSSION

We have revisited the work of Stencel & Mullan (SM80) on the location of the "velocity dividing line" (VDL) in the H-R diagram. Using updated absolute magnitudes based on *Hipparcos* data, we find that some of the earlier M_V values are altered by as much as 2–4 mag. Despite these alterations, the principal conclusion of SM80 persists: along a certain boundary in the H-R diagram, the asymmetry of the double emission peaks in Mg II h and k lines (the S/L ratio as defined by SM80) changes from solar-like (coronal, low mass loss) to nonsolar (cool massive wind).

We have compared the stars in the SM80 sample with evolutionary tracks based on various metal abundances. For stars of mass $\sim$2.5 $M_\odot$ and less, there is a clearly defined bump on the RGB when the H shell encounters a μ discontinuity. In more massive stars, there is no discernible bump, but the H shell still passes through the μ discontinuity at a certain point in time. For brevity, we refer to this point in time also as "the bump," although strictly speaking, it would be more precise to refer to the event in terms of the μ discontinuity. We find that almost all of the stars in our sample that have definitely *not* yet reached the bump have S/L > 1; i.e., the stars are not losing mass at a detectable rate. However, almost all of the stars that *have* definitely evolved through the bump have S/L < 1; i.e., these stars have massive cool winds.

Our results appear to be consistent with the following hypothesis: a cool star is not a mass loser (in the sense of the Mg II k-line asymmetry) until it reaches a stage of evolution where the H-burning shell encounters the μ discontinuity. This raises the question: why should the evolutionary event of H-shell crossing through the μ discontinuity have an effect on mass loss? In view of the earlier suggestions of Mullan (1983) and Rosner et al. (1995), we speculate that the event might be associated with an alteration in the character of the stellar dynamo. Further examination of this speculation is a topic that we postpone to a later paper.

D. J. M. acknowledges partial funding from the NASA Delaware Space Grant program and also from NASA Grant NAG5-11228.

REFERENCES

Alonso, A., Arribas, S., & Martinez-Roger, C. 1999, A&AS, 139, 335
Angulo, C., et al. 1999, Nucl. Phys. A, 656, 3
Ayres, T. R., & Johnson, H. R. 1977, ApJ, 214, 410
Ayres, T. R., Linsky, J. L., Vaiana, G. S., Golub, L., & Rosner, R. 1981, ApJ, 250, 293
Cassisi, S., & Salaris, M. 1997, MNRAS, 285, 593
Cassisi, S., Salaris, M., & Bono, G. 2002, ApJ, 565, 1231
Charbonnel, C., & do Nascimento, J. D. 1998, A&A, 336, 915
Ferraro, F. R., Messineo, M., Fusi Pecci, F., De Palo, M. A., Straneiro, O., Chieffi, A., & Limongi, M. 1999, AJ, 118, 1738
Ferraro, F. R., Montegriffo, P., Origlia, L., & Fusi Pecci, F. 2000, AJ, 119, 1282
Haisch, B. M., Schmitt, J., & Fabian, A. C. 1992, Nature, 360, 239
Henry, G. W., Fekel, F. C., Henry, S. W., & Hall, D. S. 2000, ApJS, 130, 201
Iben, I. 1968, Nature, 220, 143
Iglesias, C. A., & Rogers, F. J. 1996, ApJ, 464, 943
Jimenez, R., & MacDonald, J. 1996, MNRAS, 283, 721
Linsky, J. L., & Haisch, B. M. 1979, ApJ, 229, L27
Mullan, D. J. 1983, SAO Special Report 389, Cool Stars, Stellar Systems, and the Sun, ed. A. K. Dupree (Cambridge: Smithsonian Astrophys. Obs.), 189
———. 1984, ApJ, 284, 769
Mullan, D. J., & MacDonald, J. 2001, ApJ, 559, 353

Robinson, R. D., Carpenter, K. G., & Brown, A. 1998, ApJ, 503, 396
Rosner, R., Musielak, Z. E., Cattaneo, F., Moore, R. L., & Suess, S. T. 1995, ApJ, 442, L25
Salaris, M., Cassisi, S., & Weiss, A. 2002, PASP, 114, 375
Stencel, R. E., & Mullan, D. J. 1980a, ApJ, 238, 221
Stencel, R. E., & Mullan, D. J. 1980b, ApJ, 240, 718 (SM80)
Taylor, B. J. 1999, A&AS, 134, 523
Thomas, H. C. 1967, Z. Astrophys., 67, 420
Zoccali, M., Cassisi, S., Piotto, G., Bono, G., & Salaris, M. 1999, ApJ, 518, L49